essary, this suggests that "self-quenching" by the drug of one of the radicals may be the reason that esp A_1 cleaves DNA in a single-strand manner.

Certain of the steps leading to the activation of the warhead portion of calicheamicin have recently been investigated by NMR methods.[19] The first-order rate constant for the formation of aromatized drug from the Michael addition product outside of DNA is 5×10^{-4} s^{-1}. In addition to being second-order rate constants, the k_i' in Table I involve all of the individual steps including drug activation and the processes on DNA leading to strand breakage and thus cannot be directly compared with the rate constants of microsteps measured by NMR.

Esperamicin C and calicheamicin are unique in their DNA cleavage mechanisms. A single activation event on their chromophores leads to a double-strand break in DNA. This behavior is different from that of neocarzinostatin, which although it breaks one strand and modifies the second strand requires posttreatment of the DNA in order to produce a double-strand break.[5,7] Since esp A_1 is more potent as an antitumor agent than is esp C,[2] single- versus double-strand cleavage is not the only factor influencing cytotoxicity. Cellular uptake and drug delivery very likely also play major roles in determining the biological effectiveness of the agents.

(19) De Voss, J. J.; Hangeland, J. J.; Townsend, C. A.; *J. Am. Chem. Soc.* **1990**, *112*, 4554-4556.

Conclusions

By using a coupled kinetic model, we studied the ability of esperamicin, calicheamicin, and the enzyme DNase I to cause single- or double-strand cleavage of DNA. The analysis shows that DNase I and esperamicin A_1 cleave DNA mainly via a single-strand process, whereas esperamicin C and calicheamicin cleave mainly through a double-strand mechanism. Examination of the structure of the drugs shows that the location of the sugars on the warhead portion of the agents is a factor influencing single- versus double-strand cleavage of DNA.

Acknowledgment. We thank Drs. Golik and T. Doyle of Bristol-Myers Squibb Co. and G. Ellestad of Lederle Laboratories for helpful discussions concerning this work. We also thank the American Cancer Society, Grant NP-681, and Bristol-Myers Squibb Co. for financial support of the research.

Humidity-Controlled Reversible Structure Transition of Disodium Adenosine 5'-Triphosphate between Dihydrate and Trihydrate in a Single Crystal State

Yoko Sugawara,*,† Nobuo Kamiya,† Hitoshi Iwasaki,† Tetsuzo Ito,‡ and Yoshinori Satow§

Contribution from RIKEN (The Institute of Physical and Chemical Research), Wako, Saitama 351-01, Japan, the Kanagawa Institute of Technology, Atsugi, Kanagawa 243-02, Japan, and the Photon Factory, National Laboratory for High Energy Physics (KEK), Tsukuba, Ibaraki 305, Japan. *Received May 15, 1990*

Abstract: The humidity-controlled single-crystal transition of disodium adenosine 5'-triphosphate (Na_2ATP) between the dihydrate (**1**) and trihydrate (**2**) forms was investigated over the humidity range 5–50% at 23 °C by X-ray analysis. A crystal of **2** formed at high humidity changes into **1** at low humidity. The transition is reversible. The crystal structure of **1** was determined to be orthorhombic space group $P2_12_12_1$ with the cell parameters a = 27.572 (5), b = 21.066 (3), and c = 7.0854 (9) Å. The structure was solved by direct methods and refined to the final R value of 0.097 for 2450 independent reflections. Two water molecules, which are hydrogen-bonded to the hydroxyl groups of riboses in **2**, are lost in **1**. The triphosphate linkages are in helical arrangement, and the adenine bases are highly stacked along the c axis, as for **2**. There are two ATP molecules, A and B, in an asymmetric unit. The conformation of molecule A in **1** resembles that in **2**; the ribose is C3'-endo, and the exocyclic C4'–C5' torsion is gauche$^+$. In molecule B, the ribose is C4'-endo, and the C4'–C5' torsion is gauche$^-$, in contrast to C2'-endo–C3'-exo, and gauche$^+$ in **2**. The torsional angles around the P–O ester bonds of the triphosphate chains of both molecules in **1** differ from those in **2** by 8–47°. Conformational flexibility of ATP makes the single-crystal transition possible. The conformation of molecule B in **1** relates to the conformation of ATP in its complexes with enzymes. The crystal structure of **2** (Kennard; et al. *Proc. R. Soc. London* **1971**, *A325*, 401–436) was refined to the final R value of 0.117 with the newly collected data, and the original assignment of Na4 and OW4 was interchanged.

Introduction

Adenosine 5'-triphosphate (ATP)–enzyme interactions have been discussed with regard to the crystal structures of enzyme–ATP (or ATP analogue) complexes.[1-5] For example, in a series of site-directed mutagenic studies of tyrosyl-tRNA synthetase (TyrTS), the crystal structure of the TyrTS-tyrosyl adenylate complex was referred to in order to analyze the ATP-TyrTS interactions.[5] Although the concept of a "rigid" nucleotide was proposed based on conformational analyses of the crystal structures of nucleotides,[6] the adenosine moiety of ATP–enzyme complex is sometimes in an "uncommon" conformation; the ribose of the

†RIKEN.
‡Kanagawa Institute of Technology.
§KEK. Present address: Faculty of Pharmaceutical Sciences, University of Tokyo, Hongo, Bunkyo, Tokyo 113, Japan.

(1) (a) Monteilhet, C.; Blow, D. M. *J. Mol. Biol.* **1978**, *122*, 407–417. (b) Rubin, J.; Blow, D. M. *J. Mol. Biol.* **1981**, *145*, 489–500. (c) Brick, P.; Blow, D. M. *J. Mol. Biol.* **1987**, *194*, 287–297.
(2) (a) Banks, R. D.; Blake, C. C. F.; Evans, P. R.; Haser, R.; Rice, D. W.; Hardy, G. W.; Merrett, M.; Phillips, A. W. *Nature* **1979**, *279*, 773–777. (b) Watson, H. C.; Walker, N. P. C.; Shaw, P. J.; Bryant, T. N.; Wendell, P. L.; Fothergill, L. A.; Perkins, R. E.; Conroy, S. C.; Dobson, M. J.; Tuite, M. F.; Kingsman, A. J.; Kingsman, S. M. *EMBO J.* **1982**, *1*, 1635–1640.
(3) Shoham, M.; Steitz, T. A. *J. Mol. Biol.* **1980**, *140*, 1–14.
(4) (a) Sachsenheimer, W.; Schulz, G. E. *J. Mol. Biol.* **1977**, *114*, 23–36. Pai, E. F.; Sachsenheimer, W.; Schirmer, R. H.; Schulz, G. E. *J. Mol. Biol.* **1977**, *114*, 37–45. (b) Fry, D. C.; Kuby, S. A.; Mildvan, A. S. *Biochemistry* **1985**, *24*, 4680–4694.

0002-7863/91/1513-5440$02.50/0

Table I. Crystal Data of the Dihydrate and Trihydrate Forms of Na_2ATP

	$Na_2ATP{\cdot}2H_2O$	$Na_2ATP{\cdot}3H_2O$
crystal system	orthorhombic	orthorhombic
space group	$P2_12_12_1$	$P2_12_12_1$
a, Å	27.572 (5)	30.264 (13)
b, Å	21.066 (3)	20.816 (3)
c, Å	7.0854 (9)	7.0288 (16)
V, Å^3	4116 (1)	4428 (2)
Z	8	8
D_c, g cm^{-3}	1.895	1.816

tyrosinyl adenylate is C3′-exo in the complex with TyrTS,[1a] and the C4′–C5′ torsion of ATP is gauche$^-$ and trans in the complexes with phosphoglycerate kinase[2] and adenylate kinase,[4b] respectively. As a basis for understanding these "uncommon" conformations, the crystal structures of ATP compounds are to be referred to. However, X-ray analysis of ATP compounds has been limited only to disodium adenosine 5′-triphosphate trihydrate[7] ($Na_2ATP{\cdot}3H_2O$) and to a series of ternary complexes composed of ATP, divalent cations, and aromatic heterocyclic amines.[8] Crystals of Na_2ATP are known to exhibit variable cell dimensions, which was revealed by gravimetric analysis to originate from the diversity of the degree of hydration.[9] Therefore, high-quality Na_2ATP crystals were prepared in an attempt to elucidate the correlation between crystal structure and its hydration scheme. The preliminary finding that crystals of $Na_2ATP{\cdot}3H_2O$ (**2**) changed to $Na_2ATP{\cdot}2H_2O$ (**1**), losing water molecules, has been reported previously.[10] In the present study, the hydration–dehydration process of Na_2ATP crystals was found to be reversible and governed by relative humidity. The conformational flexibility of ATP is discussed by comparing the refined structures of these two crystal forms. Coupled with the crystal transition, which retains a single crystal state, the ATP molecules change their conformations to enable the hydrogen-bonding network to be reconstructed. The ATP conformation in **1** relates to the "uncommon" structure of ATP in its complexes with the enzymes, and a possible model of the induced fitting of ATP, from a free state in solution to a bound state in its complexes with enzymes, is provided.

Experimental Section

Crystallization. Single crystals of Na_2ATP were grown from water–1-propanol solution (1:2.5 v/v) by slow evaporation over a period of 1 month, at room temperature.

Measurements of the Humidity Dependence of Crystal Transition. A crystal of approximate size 0.01 × 0.15 × 0.35 mm^3 was mounted on a Rigaku AFC-4 four-circle diffractometer, and reflection data were collected with graphite-monochromatized Cu Kα radiation. The relative humidity surrounding the crystal was increased, in steps of approximately 10%, from 5% to 50% at 23 °C. At each humidity condition, the cell parameters were determined by a least-squares procedure on 16 reflections, and the intensities and peak profiles of representative reflections were monitored. The fluctuations of relative humidity and temperature were controlled within ±1.5% and ±0.2 °C, respectively.

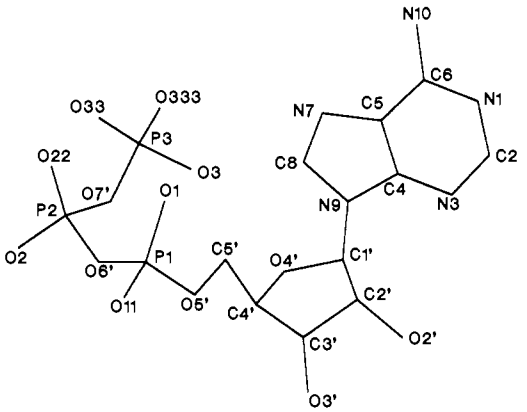

Figure 1. Atom-numbering scheme of adenosine 5′-triphosphate.

Structure Determination of $Na_2ATP{\cdot}2H_2O$ (1). Data collection of **1** was performed with the same crystal and equipment used for the humidity dependence measurements of the crystal transition. The cell parameters, refined with a least-squares procedure on 29 reflections, are listed in Table I. X-ray intensity data were collected up to a 2θ value of 126°, by the ω–2θ scan method. Variations in the structure factor amplitudes (F_o) of 3 standard reflections, which were measured every 100 reflections, were within 3%. The number of unique reflections observed with $F_o > 3\sigma(F_o)$ was 2514. The crystal was twinned, but only reflections from the main component were measured. In one spatial region, reflections from the main component and subcomponents overlapped. Therefore, 64 reflections were excluded, and the intensities and the weighting of the least-squares of the other 170 reflections in this spatial region were corrected. The data was corrected for Lorentz and polarization factors. Absorption correction (μ(Cu Kα) = 3.95 mm^{-1}) was applied according to the method of Busing and Levy.[11]

Structural analyses of **1** and **2** (vide post) were performed by the UNICS III program,[12] and the atomic scattering factors and anomalous dispersion terms were obtained from ref 13. The structure was solved by direct methods, using MULTAN78,[14] and refined by the block-diagonal least-squares method with isotropic temperature factors. One water molecule, OW6, was disordered.[15] The final R value for 2450 independent reflections was 0.097, using weights $w = [\sigma^2(F_o) + 0.005F_o^2]^{-1}$, and the highest peak in the final difference-Fourier map was 0.92 e Å^{-3}. The atom-numbering scheme is shown in Figure 1,[16] and the refined parameters are listed in Table 1s (supplementary material).

Refinement of $Na_2ATP{\cdot}3H_2O$ (2). A crystal of approximate size 0.008 × 0.2 × 0.2 mm^3 was used to collect reflection data of **2**. The cell parameters were refined by a least-squares procedure on 24 reflections and are listed in Table I. Totally, 2125 independent reflections, with $F_o > 3\sigma(F_o)$, were measured by the ω scan method to a 2θ value of 100° ($(\sin\theta)/\lambda < 0.49684$) with Cu K$\alpha$ radiation. The variations in F_o of three standard reflections were within 5%. Because the reflection intensities were very weak beyond the 2θ value of 100°, additional data were collected with use of synchrotron radiation at the Photon Factory, KEK. An automated four-circle diffractometer was used with an X-ray wavelength of 1.200 Å, which was monochromatized by double-Si(111) crystals,[17] in the ω-scan method. Through the range $70° < 2\theta < 90°$ ($0.47798 < (\sin\theta)/\lambda < 0.58926$), 941 independent reflections with $F_o > 3\sigma(F_o)$ were collected. These data were corrected for the monitored incident intensity, and then for the F_o fluctuation of three standard reflections. The variations in F_o of the three standard reflections after these corrections were less than 4%. The two sets of data, measured with

(5) Fersht, A. R.; Shi, J.-P.; Wilkinson, A. J.; Blow, D. M.; Carter, P.; Waye, M. M. Y.; Winter, G. P. *Angew. Chem.* **1984**, *23*, 467–473. Fersht, A. R.; Shi, J.-P.; Knill-Jones, J.; Lowe, D. M.; Wilkinson, A. J.; Blow, D. M.; Brick, P.; Carter, P.; Waye, M. M. Y.; Winter, G. *Nature* **1985**, *314*, 235–238. Leatherbarrow, R. J.; Fersht, A. R.; Winter, G. *Proc. Natl. Acad. Sci. U.S.A.* **1985**, *82*, 7840–7844.

(6) Rubin, J.; Brennan, T.; Sundaralingam, M. *Biochemistry* **1972**, *11*, 3112–3128. Yathindra, N.; Sundaralingam, M. *Biopolymers* **1973**, *12*, 297–314.

(7) (a) The crystal structure of $Na_2ATP{\cdot}3H_2O$ was first reported by: Kennard, O.; Isaacs, N. W.; Motherwell, W. D. S.; Coppola, J. C.; Wampler, D. L.; Larson, A. C.; Watson, D. G. *Proc. R. Soc. London* **1971**, *A325*, 401–436. (b) It was further refined with the same data: Larson, A. C. *Acta Crystallogr.* **1978**, *B34*, 3601–3604.

(8) (a) Orioli, P.; Cini, R.; Donati, D.; Mangani, S. *J. Am. Chem. Soc.* **1981**, *103*, 4446–4452. (b) Sheldrick, W. S. *Z. Naturforsch.* **1982**, *37b*, 863–871. (c) Cini, R.; Burla, M. C.; Nunzi, A.; Polidori, G. P.; Zanazzi, P. F. *J. Chem. Soc., Dalton Trans.* **1984**, 2467–2476. (d) Sabat, M.; Cini, R.; Haromy, T.; Sundaralingam, M. *Biochemistry* **1985**, *24*, 7827–7833.

(9) Lomer, T. R. *Acta Crystallogr.* **1958**, *11*, 108–110. Zeppezauer, M.; Zeppezauer, E.; Brändén, C.-I. *Acta Chem. Scand.* **1968**, *22*, 1036–1037.

(10) Sugawara, Y.; Iwasaki, H. *Acta Crystallogr.* **1984**, *A40*, C-68.

(11) Busing, W. R.; Levy, H. A. *Acta Crystallogr.* **1957**, *10*, 180–182.

(12) Sakurai, T.; Kobayashi, K. *RIKEN Hokoku* **1979**, *55*, 69–77.

(13) *International Tables for X-ray Crystallography*; Kynoch Press: Birmingham, England, 1974; Vol. IV. Sasaki, S. Anomalous Scattering Factors for Synchrotron Radiation Users, Calculated Using Cromer and Liberman's Method. Photon Factory Activity Report 83-22, 1984.

(14) Main, P.; Hull, S. E.; Lessinger, L.; Germain, G.; Declercq, J.-P.; Woolfson, M. M. *MULTAN78, A System of Computer Programs for the Automatic Solution of Crystal Structures from X-ray Diffraction Data*; Universities of York and Louvain: York, England, and Louvain, Belgium, 1978.

(15) The temperature factor of OW6 converged to a very large value, and a tentative examination of anisotropic temperature factors revealed that the large component was only β_{33}. Taking interatomic interactions into account, OW6 was treated as a pair of split atoms, OW61 and OW62, with occupancy parameters of 0.5. The distance between OW61 and OW62 is 0.9 Å.

(16) The atom-numbering scheme follows that of ref 7. One exception is that O1′ is renamed O4′.

(17) Satow, Y.; Iikaka, Y. *Rev. Sci. Instrum.* **1989**, *60*, 2390–2393.

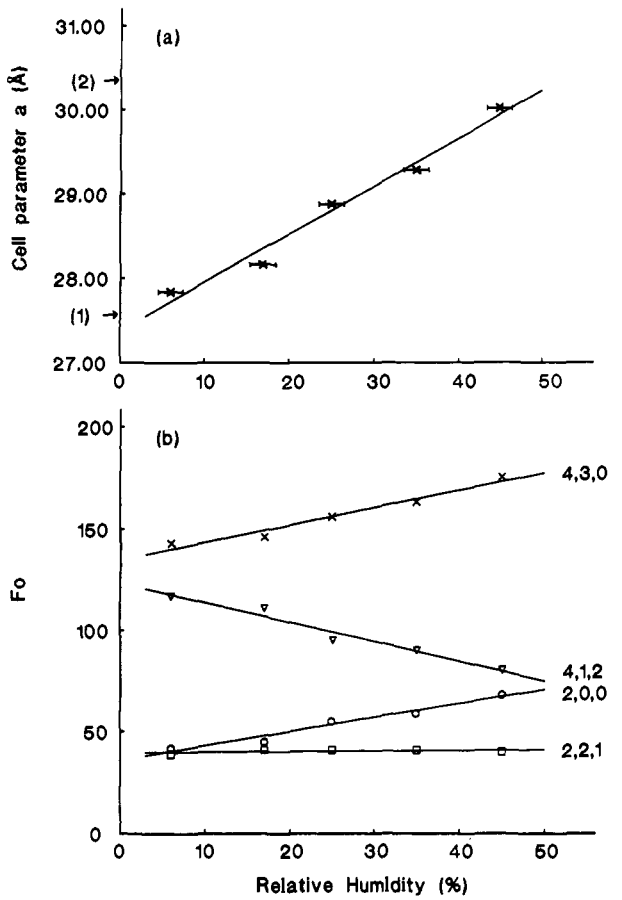

Figure 2. Plot of the cell parameter a values (a) and the structure factor amplitudes (F_o) of the representative reflections (b) against the relative humidity at 23 °C. Arrows in (a) indicate the a value of $Na_2ATP{\cdot}2H_2O$ (**1**) and $Na_2ATP{\cdot}3H_2O$ (**2**).

Cu Kα radiation and with synchrotron radiation, were corrected for Lorentz, polarization, and absorption factors (μ(Cu Kα) = 3.72 mm^{-1}, μ(1.200 Å) = 1.79 mm) individually and then put on a common scale.[18]

Refinement by the block-diagonal least-squares method was started from the reported parameters.[7] The original structure[7] was confirmed, except for the assignments of Na4 and OW4, which were interchanged on the basis of the refined interatomic distances and the correlation of the crystal structures of **1** and **2**.[19] The water molecule OW6 was disordered, there being a low peak in the electron density map at the OW61 position and the electron density being spread loosely toward the OW62 position. The final occupancy parameters of OW61 and OW62 were fixed to be 0.7 and 0.3, respectively. Refinement with isotropic temperature factors gave the final R value of 0.117 for 2923 independent reflections, using weights $w = [\sigma^2(F_o) + 0.003F_o^2]^{-1}$. The highest peak observed in the final difference-Fourier map was 1.12 e Å^{-3}. In the previous studies, the refinements were carried out under constraints to supplement the insufficient data.[7] In this study, all interatomic distances and bond angles could be refined to chemically reasonable values without constraints. These refined atomic parameters are listed in Table 1s.

Results

Characteristics of the Crystal Transition of Na_2ATP between the Dihydrate (1) and Trihydrate (2) Forms. The cell parameter values of Na_2ATP depend on relative humidity (rh). A plot of the equilibrium value of cell parameter a against relative humidity, determined by successive measurement in the relative humidity range from 5 to 50%, is shown in Figure 2a. As a first approximation, the cell parameters a, b, and c change linearly.

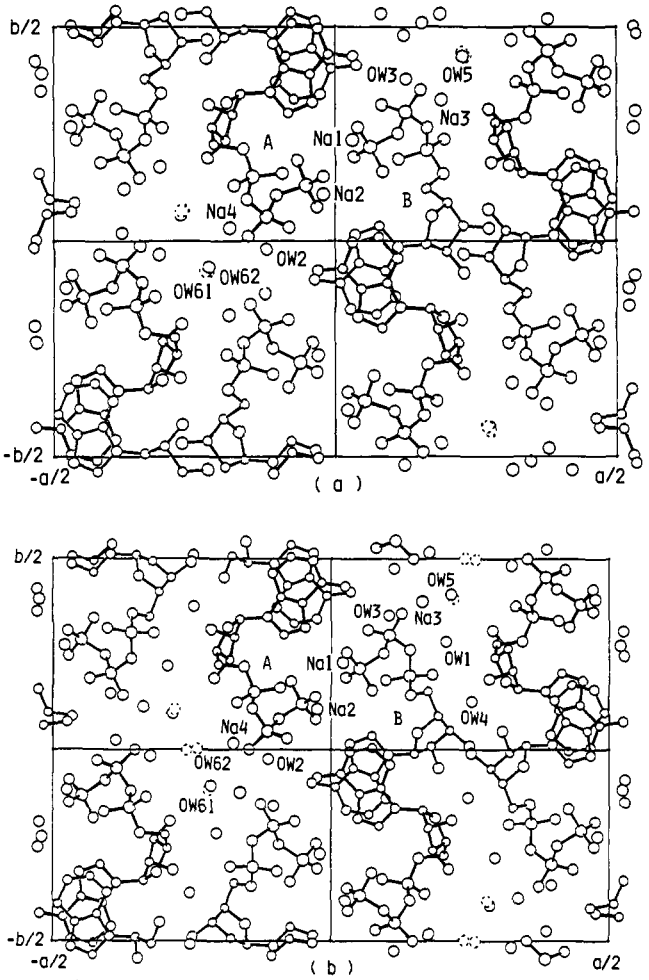

Figure 3. Crystal structures of the dihydrate and trihydrate forms of Na_2ATP viewed along the c axis. The disordered water molecules are shown in dotted circles: (a) $Na_2ATP{\cdot}2H_2O$, (b) $Na_2ATP{\cdot}3H_2O$.

Coupled with the humidity change from 5% to 50%, cell parameter a lengthens by about 10% and b and c shorten by about 1% (Table I). The process was confirmed to be reversible. A crystal with the cell parameters at approximately 5% rh was determined to be $Na_2ATP{\cdot}2H_2O$,[10] and the cell parameters at approximately 50% rh coincide with the reported values of $Na_2ATP{\cdot}3H_2O$.[7]

The plots of the structure factor amplitudes (F_o) of representative reflections against relative humidity are shown in Figure 2b. In the course of the transition, their changes are continuous. Neither splitting nor marked line broadening of reflection peaks was observed. The space group $P2_12_12_1$ remained unchanged.

Crystal Structure of $Na_2ATP{\cdot}2H_2O$ (1). The crystal structure of **1** is shown in Figure 3a. Although it is closely related to that of **2** (Figure 3b), there is one prominent difference. Out of six symmetrically independent water molecules in **2**, OW1 and OW4 do not exist in **1**.[20] Lack of these water molecules couples with reduction of the space between molecules A and B at $x = {}^1/_4$. As a result, cell parameter a of **1** is shorter than that of **2** by 2.7 Å.

There are three common characteristics in the crystal structures of **1** and **2**:[7] the stacking structure of adenine bases, the helical arrangement of pyrophosphate linkages, and the pseudoinversion symmetry. The adenines of molecules A and B stack alternately along the c axis with a spacing of 3.3–3.4 Å. The mode of stacking shows little change during the crystal transition.[21] The helices

(18) The R value for the scaling procedure ($\sum(|F_{hl} - G_l F_h|)/\sum F_{hl}$) was 0.05, where F_{hl} is the observed structure factor of reflection h in the lth set, G_l is the scaling factor for the lth set, and F_h is the averaged structure factor of reflection h, after the scaling procedure.

(19) In **1** no peak corresponding to OW4 (original Na4) exists, and the position of Na4 in **1** is very near to the position of Na4 (original OW4) in **2**. In addition, the shortest distance between Na4 and the coordinating oxygen atom is 2.30 Å, which is too short for an O–H···O hydrogen bond.

(20) OW4 was assigned to Na4 in the previous studies.[7] Concerning the change of assignments, see the Experimental Section and ref 19.

(21) The angle between two mean planes of successively stacked adenine bases is 178.3 (5)° in **1** and 179.3 (4)° in **2**. The minimum distances from the adenine atoms of molecule A to the mean planes of adjacent adenines of molecule B are 3.26 (2) (from C6A to the upper adenine) and 3.36 (2) Å (from C4A to the lower one) in **1** and 3.28 (2) (from N9A to the upper one) and 3.29 (2) Å (from C2A to the lower one) in **2**.

Table II. Sodium Coordination Distances and Hydrogen-Bond Distances (Å) with Estimated Standard Deviations in Parentheses[a]

$Na_2ATP·2H_2O$				$Na_2ATP·3H_2O$			
Sodium Coordination Distances							
Na1	O333A	1[b]	2.33 (2)	Na1	O333A	1	2.39 (2)
	N7A	1	2.69 (2)		N7A	1	2.81 (2)*
	O1B	1	2.48 (2)		O1B	1	2.55 (2)
	O22B	1	2.41 (2)		O22B	1	2.44 (2)
	O33B	2	2.81 (2)*		O33B	2	2.63 (2)
	O333B	1	2.41 (2)		O333B	1	2.44 (2)
Na2	O1A	1	2.32 (2)	Na2	O1A	1	2.38 (2)
	O22A	1	2.53 (2)		O22A	1	2.44 (2)
	O33A	3	2.89 (2)*		O33A	3	2.61 (2)
	O333A	1	2.39 (2)		O333A	1	2.33 (2)
	O333B	1	2.39 (2)		O333B	1	2.33 (2)
	N7B	1	2.52 (2)		N7B	1	2.59 (2)
Na3	O11B	3	2.30 (2)	Na3	O2B	1	2.36 (2)
	O2B	1	2.34 (2)		OW1	1	2.58 (3)
	O3'A	7	2.48 (2)		O2A	11	2.42 (2)
	OW3	11	2.36 (2)		OW3	11	2.26 (3)
	OW61	11	2.56 (3)		OW61	11	2.68 (7)
	OW62	11	2.57 (3)				
Na4	O11A	2	2.34 (2)	Na4	O11A	2	2.62 (4)
	O2A	1	2.38 (2)		O2A	1	2.50 (4)
	OW61	6	2.49 (3)		OW61	1	2.68 (8)
	OW62	6	2.51 (3)		OW62	1	2.90 (20)*
	OW2	12	2.32 (2)		OW62	6	2.94 (20)*
	OW5	12	2.41 (3)		OW2	12	2.30 (4)
Hydrogen-Bond Distances[c]							
O3A	O1A	2	2.56 (2)	O3A	O1A	2	2.50 (2)
O2'A	O11B	8	2.79 (2)	O2'A	OW4	8	2.78 (3)
				O2'A	O2'B	10	2.97 (2)
O3'A	O11A	2	2.68 (2)	O3'A	O11A	2	2.69 (2)
N1A	O33A	10	2.56 (2)	N1A	O33A	10	2.62 (2)
N10A	O22B	1	2.82 (2)	N10A	O22B	1	2.77 (2)
N10A	OW2	1	3.07 (3)	N10A	OW2	1	2.96 (3)
N10A	O33A	10	3.11 (3)	N10A	O33A	10	3.16 (2)
O3B	O1B	3	2.54 (2)	O3B	O1B	3	2.57 (2)
O2'B	O2'A	12	2.68 (2)	O2'B	O3'B	5	2.66 (3)
O3'B	O4'A	7	3.33 (2)*	O3'B	OW4	4	2.80 (3)
O3'B	N3A	7	3.25 (2)*				
N1B	O33B	13	2.57 (2)	N1B	O33B	13	2.60 (2)
N10B	O22A	1	2.83 (3)	N10B	O22A	1	2.79 (2)
N10B	OW3	1	2.94 (3)	N10B	OW3	1	2.92 (3)
N10B	O33B	13	3.08 (2)				
				OW1	O11B	3	2.72 (3)
				OW1	O3'A	7	3.05 (3)
OW2	O2B	1	2.84 (2)	OW2	O2B	1	2.79 (3)
OW2	O22A	11	2.88 (2)	OW2	O22A	11	2.77 (3)
OW3	O2A	1	2.91 (3)				
OW3	O22B	12	2.91 (2)	OW3	O22B	12	2.91 (3)
				OW4	O11B	1	2.68 (3)
				OW4	O4'A	7	2.88 (2)
OW5	O2B	1	2.87 (3)	OW5	O2B	1	2.95 (5)
				OW5	O3'A	7	2.86 (5)
OW61	O2A	1	2.82 (4)	OW61	OW5	12	2.66 (8)
OW61	O11A	6	2.80 (4)				
OW62	O2A	1	2.96 (4)	OW62	O2A	1	2.80 (19)
OW62	OW5	13	3.04 (4)	OW62	OW5	9	2.53 (19)

[a] Although distances marked with an asterisk are a little longer than effective interactions, they are listed for the sake of comparison between the dihydrate and trihydrate. [b] Operation codes: 1, x, y, z; 2, $x, y, z-1$; 3, $x, y, z+1$; 4, $-x+{}^1/_2, -y, z+{}^1/_2$; 5, $-x+{}^1/_2, -y, z-{}^1/_2$; 6, $-x-{}^1/_2, -y, z-{}^1/_2$; 7, $x+{}^1/_2, -y+{}^1/_2, -z+1$; 8, $x-{}^1/_2, -y+{}^1/_2, -z$; 9, $x-{}^1/_2, -y+{}^1/_2, -z+1$; 10, $-x, y+{}^1/_2, -z+{}^1/_2$; 11, $-x, y+{}^1/_2, -z+{}^3/_2$; 12, $-x, y-{}^1/_2, -z+{}^1/_2$; 13, $-x, y-{}^1/_2, -z+{}^3/_2$. [c] Estimated hydrogen donors are listed at the left side.

of triphosphate linkages continue along the c axis mediated by hydrogen bonds between O3–H and O1 of the neighboring molecules and by coordinations between sodium ions Na1 and Na2 and acidic oxygens O1, O22, O333, and O33 (see Table II). The pseudosymmetry in **1**, the center of which is at $x = 0.0$, $y = 0.17$, and $z = 0.50$, is far better than that in **2**. Molecule A and molecule B, Na1 and Na2, Na3 and Na4, OW2 and OW3, and OW5 and the middle point between OW61 and OW62 are related by the pseudoinversion in both their positions (Table 1s) and interactions with neighbors (Table II).

Sodium Coordinations and Hydrogen-Bonding Schemes of $Na_2ATP·2H_2O$ (1). The sodium coordinations and hydrogen-bond distances are shown in Table II. The sodium ions are classified into two groups. Na1 and Na2 are tightly bound to the triphosphate chains, and the coordination scheme around them in **1** is common to that in **2**. Na3 and Na4 are coordinated by both anionic oxygens of phosphates and water molecules, and the coordination schemes in **1** and **2** are different.

The water molecules are classified into three groups. The water molecules of the first group, OW2 and OW3, interact with the anionic phosphate oxygens, the amino groups of adenines, and the sodium ions. Their coordination and hydrogen-bonding schemes in **1** are common to those in **2**. The water molecules of the second group, OW1 and OW4, exist only in **2**. They are hydrogen-bonded to the hydroxyl groups of the riboses in **2**. Conformational changes of the riboses are induced by their loss (vide post). The water molecules of the third group, OW5, OW61, and OW62, play two roles: They fill a channel along the c axis at $x = {}^1/_4$, $y = {}^1/_2$ in an asymmetric unit and solvate sodium ions.

To compensate the interactions mediated by OW1 and OW4 in **2**, direct interactions between O2A′ and O11B, Na3 and O3′A, and Na3 and O11B are formed in **1**. In addition, Na4 and OW61 at $(-x-{}^1/_2, -y, z-{}^1/_2)$ are within interactive distance in **1**. So are Na4 and OW62. The temperature factors of Na4, OW5, OW61, and OW62 are near 20 Å^2 in **2**, and they are highly disordered. In the crystal structure of **1**, coordinations around Na3, Na4, OW5, OW61, and OW62 are far tighter, and the temperature factors of these atoms range between 2.8 and 5.6 Å^2.

Molecular Structure of ATP in $Na_2ATP·2H_2O$ (1) and Conformational Differences between the Two Hydrates. The Bond lengths and bond angles of ATP in both hydrates (Table 2s), including those of the triphosphate chains (Table III), are within 3 times the estimated standard deviations (3σ) from the mean values of related compounds.[22,23]

The main torsional angles of the ATP molecules in **1** and **2** are listed in Table IV. Conformational changes are introduced both in the triphosphate chains and in the adenosine moieties by the crystal transition. The torsional angles around the P–O ester bonds, $\omega 2$, $\omega 3$, and $\omega 4$, in the two hydrates differ by 8–47°. The pseudoinversion symmetry of the crystal structure was mentioned in the previous section. Comparing the torsional angles in Table IV, we note that the pseudosymmetry between the pyrophosphate moieties of molecules A and B in **1** is far better than that in **2**; the corresponding angles in **1** are nearly equal with reversed signs. The conformation around the P–P axis of a nucleotide is known to prefer the staggered form.[24] The staggered relationship is satisfied in both crystal forms except that around the P1–P2 of molecule B in **2** (Table 3s). The P1–P2 of molecule B is the all-trans eclipsed arrangement[23] in **2** and alters toward the staggered arrangement in **1**.

The adenosine moiety of molecule A in **1** is anti around the glycosidic bond, C3′-endo at the ribose, and gauche$^+$ around the C4′–C5′ bond. The conformation of this portion is essentially the same as that in **2**. On the other hand, the conformation of molecule B in **1** is remarkably different from that in **2**. Molecule B is anti around the glycosidic bond ($\chi = 4°$), C4′-endo ($P = 233°$) at the ribose part, and gauche$^-$ arund the C4′–C5′ bond in **1**. It is anti ($\chi = 29°$), C2′-endo–C3′-exo ($P = 177°$), and gauche$^+$ in **2**. Coupled with the conformational change around the C4′–C5′ bond, the torsional angle around the O5′–P1 bond ($\omega 1$) is 75° in **1**, in contrast to −45° in **2**.

The molecules A and B in an asymmetric unit of **1** are superimposed on those of **2** (Figure 4a,b). Molecule A and the β- and γ-phosphate portions of molecule B in **1** and in **2** overlap well

(22) Tayler, R.; Kennard, O. *J. Mol. Struc.* **1982**, *78*, 1–28. Murray-Rust, P.; Motherwell, S. *Acta Crystallogr.* **1978**, *B34*, 2534–2546. Bartenev, V. N.; Kameneva, N. G.; Lipanov, A. A. *Acta Crystallogr.* **1987**, *B43*, 275–280.
(23) Saenger, W. *Principles of Nucleic Acid Structure*; Springer-Verlag: New York, Berlin, Heidelberg, Tokyo, 1983.
(24) Sundaralingam, M. *Biolopymers* **1969**, *7*, 821–860.

Table III. Bond Lengths (Å) and Angles (deg) of the Triphosphate Portions with the Mean Values of Nucleotides[a]

	mean[b] value	$Na_2ATP·2H_2O$ A	$Na_2ATP·2H_2O$ B	$Na_2ATP·3H_2O$ A	$Na_2ATP·3H_2O$ B
		Bond Lengths			
P1–O1	1.49 (3)	1.49 (2)	1.51 (2)	1.47 (2)	1.47 (2)
P1–O11	1.48 (2)	1.47 (2)	1.50 (2)	1.49 (2)	1.45 (2)
P1–O6′	1.63 (2)	1.60 (2)	1.61 (2)	1.62 (2)	1.60 (1)
P1–O5′	1.59 (1)	1.57 (2)	1.57 (2)	1.61 (2)	1.58 (2)
P2–O6′		1.61 (2)	1.58 (2)	1.56 (2)	1.61 (1)
P2–O2		1.47 (2)	1.48 (2)	1.48 (2)	1.50 (2)
P2–O22		1.47 (2)	1.47 (2)	1.49 (2)	1.46 (2)
P2–O7′		1.54 (2)	1.59 (2)	1.58 (2)	1.60 (2)
P3–O7′	1.59 (2)	1.63 (2)	1.63 (2)	1.58 (2)	1.63 (2)
P3–O3	1.58 (4)	1.53 (1)	1.56 (2)	1.54 (2)	1.57 (1)
P3–O33	1.47 (5)	1.49 (2)	1.47 (2)	1.48 (2)	1.50 (1)
P3–O333	1.44 (3)	1.47 (2)	1.50 (2)	1.48 (2)	1.47 (1)
		Bond Angles			
O1–P1–O11	118 (1)	119 (1)	121 (1)	119 (1)	122 (1)
O1–P1–O6′	110 (2)	112 (1)	109 (1)	110 (1)	111 (1)
O1–P1–O5′	110 (2)	105 (1)	109 (1)	107 (1)	106 (1)
O11–P1–O6′	108 (2)	103 (1)	108 (1)	109 (1)	102 (1)
O11–P1–O5′	109 (1)	112 (1)	108 (1)	111 (1)	111 (1)
O6′–P1–O5′	99 (2)	106 (1)	101 (1)	99 (1)	104 (1)
O6′–P2–O2		104 (1)	105 (1)	107 (1)	105 (1)
O6′–P2–O22		109 (1)	110 (1)	111 (1)	111 (1)
O6′–P2–O7′		104 (1)	102 (1)	99 (1)	102 (1)
O2–P2–O22		119 (1)	119 (1)	120 (1)	116 (1)
O2–P2–O7′		109 (1)	107 (1)	107 (1)	108 (1)
O22–P2–O7′		111 (1)	113 (1)	111 (1)	114 (1)
O7′–P3–O3	103 (2)	99 (1)	100 (1)	102 (1)	99 (1)
O7′–P3–O33	106 (2)	108 (1)	107 (1)	105 (1)	106 (1)
O7′–P3–O333	112 (1)	109 (1)	108 (1)	108 (1)	110 (1)
O3–P3–O33	107 (4)	110 (1)	111 (1)	110 (1)	110 (1)
O3–P3–O333	109 (1)	110 (1)	110 (1)	111 (1)	111 (1)
O33–P3–O333	119 (3)	119 (1)	119 (1)	120 (1)	119 (1)
P1–O6′–P2		133 (1)	137 (1)	134 (1)	132 (1)
P2–O7′–P3	131 (2)	135 (1)	136 (1)	139 (1)	134 (1)
P1–O5′–C5′	121 (2)	119 (1)	113 (1)	120 (1)	122 (1)

[a] Estimated standard deviations are in parentheses. [b] Mean values obtained by statistical analyses of nucleotides.[22,23]

with each other. The ribose and the α-phosphate portions of molecule B, however, deviate greatly, and the adenine base of molecule B shifts along the *c* axis as a result of the conformational change.

Discussion

Single-Crystal Transition of Na_2ATP. Na_2ATP crystals are known to have various cell dimensions,[9] and the origin was discussed on the basis of the crystal structure of $Na_2ATP·3H_2O$.[7] The present study reveals that relative humidity controls the reversible single-crystal transition of Na_2ATP between the dihydrate and trihydrate forms.

The crystal lattice is often destroyed by structural or compositional changes. However, there are some special cases where a single crystal state is retained during transition. Judging from the results that the conformational changes of ATP are coupled with the transition, and that the two water molecules, which are lost in **1**, are firmly netted in the hydrogen-bonding scheme in **2**, the crystal transition of Na_2ATP is to be classified into the category of topochemical reactions[25] rather than that of zeolites.[26]

An intermediate stage during the single-crystal transition may be described by the following three models. The first, the mixture model, is that microcrystals of **1** and **2** coexist in one crystal, and their relative amounts change during the transition. The second, the transition structure model, is that the specific structure exists at each intermediate stage. The third, the disorder model, is that the structure at each intermediate stage is to be described as a disorder of **1** and **2**. The observations that the diffraction peaks do not split at an intermediate stage exclude the first mixture model. Tentative analysis of one intermediate stage[27] revealed that electron density is generally diffuse at the parts where the conformational differences between **1** and **2** are prominent and that the structure at this stage corresponds approximately to an average structure of **1** and **2**. These results are poorly explained by the second transition structure model but are more reasonably explained by the third disorder model.[28]

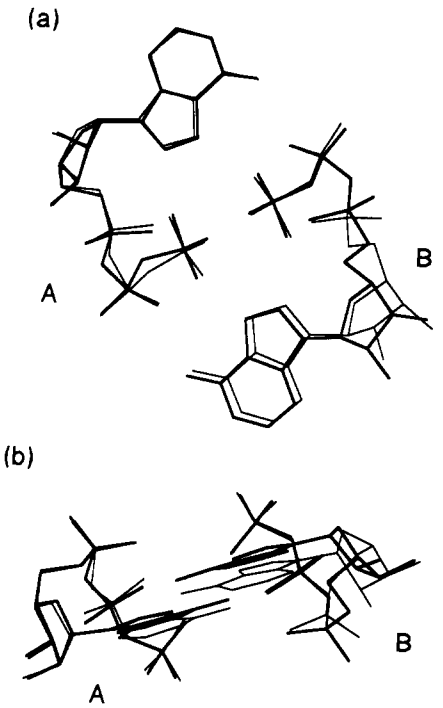

Figure 4. Molecules A and B in an asymmetric unit of $Na_2ATP·2H_2O$ (shown in heavy lines), superimposed on those of $Na_2ATP·3H_2O$. The latter coordinates are shifted by +0.20, +0.15, −0.35 Å along the *a*, *b*, and *c* axes, respectively: (a) projection on the *ab* plane, (b) projection on the *ac* plane.

Conformational Flexibility of ATP Molecules. The crystal transition of Na_2ATP reminds us of the polymorphism of nucleic acids, e.g., the A–B transition coupled with water activity.[23] Although the helical structure in **1** and **2** is made of triphosphate linkages and is different from that of nucleic acids, which consists of covalent bonds between phosphates and riboses, the transition scheme is quite similar. The base-stacking structure and the helices maintain the highly ordered structure. The torsional angles of χ, φ, and ψ and the ribose puckering conformation act to relax the distortion and to reconstruct hydrogen-bonding networks. It was an unexpected result that OW1 and OW4, which have sufficient interactions with surrounding atoms in **2**, are lost in **1**, whereas OW5, OW61, and OW62, whose temperature factors are abnormally large in **2**, remain in **1**. This phenomenon can be explained by the cooperative effects of the following two factors: The binding energy of water with anionic oxygen atoms of phosphates and sodium ions is larger than that with hydroxyl groups of riboses,[30] and hydroxyl groups of riboses have high flexibility to reconstruct a new hydrogen-bonding network.[31] Coupled with the transition, the coordination scheme around the sodium ions of Na3 and Na4 is also changed. This is the first example where drastic conformational change of the nucleotide

(25) Ohashi, Y. *Acc. Chem. Res.* **1988**, *21*, 268–274, and references therein.

(26) Breck, D. W. *J. Chem. Educ.* **1964**, *41*, 678–689. In the case of zeolites, the framework structure does not change during the reversible gain or loss of ions and small molecules.

(27) Sugawara, Y.; Ito, T.; Kamiya, N.; Iwasaki, H.; Satow, Y. *Acta Crysatallogr.* **1987**, *A43*, C-50.

(28) In topochemical reactions, intermediate stages were mostly analyzed as disordered structures. Judging from the crystal structures of the two hydrates, an intermediate stage may correspond to a partially ordered layer structure, a theoretical treatment of which was presented by Hendricks and Teller.[29]

(29) Hendricks, S.; Teller, E. *J. Chem. Phys.* **1942**, *10*, 147–167.

(30) Texter, J. *Prog. Biophys. Mol. Biol.* **1978**, *33*, 83–97.

(31) Levitt, M.; Warshel, A. *J. Am. Chem. Soc.* **1978**, *100*, 2607–2613.

Table IV. Phase Angle of Pseudorotation of the Ribose (P) and Main Torsional Angles (deg)[a]

		χ	P	ψ	ϕ	$\omega 1$	$\omega 2$	$\omega 3$	$\omega 4$
$Na_2ATP{\cdot}2H_2O$[b]	A	61	11	60	−146	67	105	−72	127
	B	4	233	−67	−158	75	−119	82	−126
$Na_2ATP{\cdot}3H_2O$[b]	A	64	5	56	−139	72	152	−117	88
	B	29	177	57	−141	−45	−76	62	−118
ZnATP(bpy)[c]	A	38	11	64	−130	−54	−71	−106	85
	B	−8	20	54	154	53	89	95	−67
CuATP(phen)[d]	A	32	16	60	−147	−55	−71	−109	77
	B	6	15	50	170	72	85	99	−75
MgATP(bipyam)[e]		67	179	57	168	−66	159	67	−101
CaATP(bipyam)[f]		58	156	46	172	−58	162	60	−97
MnATP(bipyam)[g]		66	179	55	171	−66	161	64	−100

[a] Phase angles of pseudorotation, P, are calculated following the definition given in ref 34. Torsional angles: χ, C8–N9–C1′–O4′; ψ, C3′–C4′–C5′–O5′; ϕ, C4′–C5′–O5′–P1; $\omega 1$, C5′–O5′–P1–O6′; $\omega 2$, O5′–P1–O6′–P2; $\omega 3$, P1–O6′–P2–O7′; $\omega 4$, O6′–P2–O7′–P3. [b] This work. [c] [Zn(H_2ATP)(2,2′-bipyridine)]$_2{\cdot}4H_2O$.[8a] [d] [Cu(H_2ATP)(1,10-phenanthroline)]$_2{\cdot}7H_2O$.[8b] [e] [$Mg(H_2O)_6$][Hbis(2-pyridyl)amine]$_2$[$Mg(HATP)_2$]$\cdot 12H_2O$.[8c] [f] [$Ca(H_2O)_6$][Hbis(2-pyridyl)amine]$_2$[$Ca(HATP)_2$]$\cdot 9H_2O$.[8c] [g] [$Mn(HATP)_2$][$Mn(H_2O)_6$][Hbis(2-pyridyl)amine]$_2\cdot 12H_2O$.[8d]

couples with the hydration–dehydration process in a crystal state.[32] The crystal transition of Na_2ATP presents a prototye of the transformation of nucleic acids, which accompanies the changes of hydration and coordination schemes.

Comparing the conformations of ATP in Na_2ATP crystals with those of other ATP compounds (Table IV), we note that the conformation of molecule B in **1**, i.e., C4′-endo (P = 233°) and gauche$^-$ (ψ = −67°), is unique.[34] Indeed, riboses of nucleotides and nucleosides are seldom in the C4′-endo conformation, except for a few examples such as cyclic uridine 3′,5′-phosphate[35a] and cyclic cytidine 2′,3′-phosphate,[35b] which have an extra yoke. Here it should be noted that C4′-endo and gauche$^-$ are closely related.[36] The gauche$^-$ form (or the trans form) is necessary for the C4′-endo conformation to avoid the too short distance between C8 and O5′.[37] The χ angle is also correlated with the ribose conformation.[38] The conformation energy map, P against χ, for a nucleoside calculated by the quantum mechanical method has a shallow minimum at the C4′-endo and χ = 0° region,[39] in agreement with the observed conformation (χ = 4°) of molecule B in **1**. In the case of $Na_2ATP{\cdot}2H_2O$, requirements of the hydrogen-bond formation and of the crystal packing may induce the ribose to be C4′-endo, which would accompany the changes of the χ and the ψ angles.

Specific interactions between proteins and ligands often cause conformational changes of ligands as well as proteins, which are essential for biological functions. The conformation of molecule B is of interest relative to that of ATP bound to proteins. In the phosphoglycerate kinase–ATP complex, ATP takes the gauche$^-$ conformation around the C4′–C5′ bond as molecule B, although the ribose is in the common C3′-endo[2a] or C2′-endo[2b] conformation. One other noteworthy example is the tyrosinyl adenylate–TyrTS complex in which tyrosinyl adenylate, an analogue of the intermediate product from ATP and tyrosine, is C3′-exo at the ribose and gauche$^-$ around the C4′–C5′ bond.[1a] The C3′-exo conformation is situated at the midpoint of the pseudorotation path from C2′-endo to C4′-endo, i.e., from the conformation of molecule B in **2** to that in **1**. The gauche$^-$ conformation around the C4′–C5′ bond, which is shared by molecule B in **1**, is significant because it is closely related to the attacking direction of the carboxyl group of tyrosine at the reaction center. On the analogy of the crystal transition of Na_2ATP, the modification of TyrTS by the site-directed mutagenesis[5] may induce changes in the binding conformation of the substrate as well as in the binding energy, which would increase or decrease the reactivity. From these examples, we conclude that the conformational change in Na_2ATP crystals can be regarded as a basic model for induced fitting of ATP in ATP–enzyme complexes and is instructive for considering ATP–protein interactions.

Conclusions

A part of the water molecules of Na_2ATP crystals are found to be in equilibrium with water vapor in the atmosphere. Coupled with the hydration–dehydration process, conformational changes of ATP are induced. It is characteristic that a single crystal state is retained during the transition. By the structure analyses of the dihydrate and trihydrate forms of Na_2ATP, the dynamic aspect of ATP conformation is revealed, which is useful for understanding ATP–enzyme interactions. We carried out the structure analyses under the condition of relative humidity up to 50%. It is of interest to see how Na_2ATP changes its structure above 50% relative humidity. A similar reversible crystal transition coupled with the hydration–dehydration process is observed in the case of guanosine crystals.[40] Transitions of this type probably occur in other nucleoside and nucleotide crystals and will offer valuable information on the dynamic structure of not only ATP but also nucleic acids.

Acknowledgment. This work was partly supported by Grant No. 63628007 from the Ministry of Education, Science and Culture of Japan. The experiments at the Photon Factory, KEK, were performed under the approval of the Photon Factory Program Advisory Committee (Proposal No. 86-033). All calculations were made by a FACOM M780 computer of RIKEN.

Supplementary Material Available: Table 1s, fractional coordinates and isotropic temperature factors of $Na_2ATP{\cdot}2H_2O$ and $Na_2ATP{\cdot}3H_2O$, Table 2s, bond lengths and angles of $Na_2ATP{\cdot}2H_2O$ and $Na_2ATP{\cdot}3H_2O$ with the mean geometry of nucleotides, Table 3s, torsional angles along the P–P axes (7 pages); tables of observed and calculated structure factors of the dihydrate and trihydrate (19 pages). Ordering information is given on any current masthead page.

(32) Although the hydration–dehydration process of nucleotide crystals has already been reported,[33] there has been no evidence of a dynamical change of molecular conformation.

(33) Falk, M.; Hartman, K. A., Jr.; Load, R. C. *J. Am. Chem. Soc.* **1962**, *84*, 3843–3846. Nagashima, N. Doctoral Dissertation, University of Tokyo, 1985.

(34) Referring to the conformational analyses of 60 nucleotides and nucleosides made by Altona and Sundaralingam, no example exists in the region from C4′-endo to C2′-exo along pseudorotation pathway of the furanose ring, and only three examples take gauche$^-$. Altona, C.; Sundaralingam, M. *J. Am. Chem. Soc.* **1972**, *94*, 8205–8212.

(35) (a) Coulter, C. L. *Acta Crystallogr.* **1969**, *B25*, 2055–2065; *Ibid.* **1970**, *B26*, 411. (b) Coulter, C. L.; Greaves, M. L. *Science* **1970**, *169*, 1097–1098.

(36) Westhof, E.; Sundaralingam, M. *J. Am. Chem. Soc.* **1980**, *102*, 1493–1500.

(37) If the conformation around the C4′–C5′ bond of molecule B in **1** was gauche$^+$, the interatomic distance between O5′ and C8 would be 2.3 Å, which is too short for a van der Waals contact.

(38) If the χ angle of molecule B in **1** was the same as that in **2** (χ = 29°), the distance between C5′ and C8 would be 2.9 Å.

(39) Saran, A.; Perahia, D.; Pullman, B. *Theor. Chim. Acta (Berlin)* **1973**, *30*, 31–44.

(40) Sugawara, Y.; Iimura, Y.; Iwasaki, H.; Saitô, H.; Urabe, H. To be submitted for publication.